Optical and Quantum Electronics **23** *(1991) S477–S484*

Measurement of spatial coherence of a copper vapour laser beam using a reversal shear interferometer

T. OMATSU, K. KURODA, T. SHIMURA, K. CHIHARA, M. ITOH, I. OGURA
Institute of Industrial Science, University of Tokyo, Roppongi, Minatoku, Toyko, 106 Japan

Received 21 March; revised 22 June; accepted 2 July 1990

We measured the spatial coherernce of a copper vapour laser (CVL) beam with an unstable resonator by the reversal shear interferometer. By this method, we can evaluate the spatial coherence function from a single-shot measurement. The spatial coherence width was 5 mm when an unstable resonator with a magnification factor of 60 was used. Moreover we verified the result by the theoretical calculation on the basis of the passive resonator model.

1. Introduction

The copper vapour laser (CVL) is a high average power and high repetition rate (≈ 4 kHz) pulse laser at 510.6 nm and 578.2 nm [1]. The second harmonics of the CVL beam at 255.3 nm will be a high average and high repetition rate ultraviolet (UV) light [2, 3, 4]. We have carried out the second harmonic generation of the CVL, using barium borate as a nonlinear crystal, and have achieved a conversion efficiency of 9% [3].

In the second harmonic generation, the maximum conversion efficiency depends on the spatial coherence of the light source. In general the high power pulse lasers, such as the CVL, radiate partially coherent light [5, 6, 7]. Thus measuring the spatial coherence of the CVL beam is important for estimating the maximum efficiency.

The degree of spatial coherence can be measured by using Young's interferometer [8]. But in this method we must measure the visibility of the fringes by varying a double pinhole spacing to find the coherence width, which is defined as the double pinhole spacing at which the visibility becomes zero. Moreover, since the fringe period depends on the double pinhole spacing, we have to control the imaging magnficiation shot by shot on the detector surface. Therefore it takes a long time to measure the spatial coherence function.

In this paper we report the measurement of the spatial coherence of the CVL beam by the reversal shear interferometer, by which we can evaluate the spatial coherence function from a single shot measurement.

2. Reversal shear interferometer

It has been reported that the reversal shear interferometer [9, 10] has been successfully used for high sensitivity tilt measurement.

0306-8919/91 $03.00 + .12

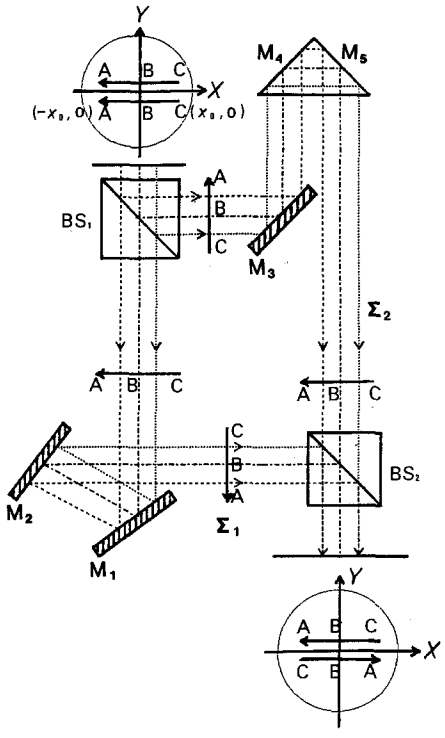

Figure 1 The reversal shear interferometer BS_1, BS_2: the prism beam splitters.

Murty's reversal shear interferometer is basically a Twyman–Green interferometer, but a mirror in one arm is replaced by a roof prism, which reverses a reflected beam horizontally. However it is impossible to observe a interference fringe around the folding axis because light cannot return from the edge of the roof prism.

We propose a new type of reversal interferometer. This interferometer is illustrated in Fig. 1. The laser beam is divided into two beams by a beam splitter BS_1. The laser beam propagating in the optical path Σ_1 is reflected twice, at mirrors M_1 and M_2. The laser beam propagating in the path Σ_2 is reflected three times, at mirrors M_3, M_4 and M_5. Therefore the wavefront CBA from Σ_2 is a folding around the y axis of the wavefront ABC from Σ_1. These two wavefronts make interference fringes on the screen after passing the beam splitter BS_2. For cancelling the difference of the optical path lengths between Σ_1 and Σ_2, we inserted a roof prism RP.

On the y axis of the observation plane, we observe the interference between the point B of ABC and the point B of CBA. Since both are originally the same point, the shear is zero. On the other hand, at the point A(C), the point A(C) of ABC interferes with the point C(A) of CBA. The shear between two points is $\overline{AC}$. Therefore we can observe the fringes, in which the shear varies continuously from the y axis to the edge along the x axis. Let the x coordinate of A and C of the original wavefront ABC be x_0 and $-x_0$. The shear $S(=\overline{AC})$ of the interference fringe on the point A(C) is

$$S = 2x_0 \tag{1}$$

When the visibility of the fringe is measured from the y axis to the edge along the x axis, we can obtain the spatial coherence function at once.

3. Experiment

The CVL used in this experiment was operated at a repetition frequency of 4 kHz with a positive confocal type unstable resonator [11]. We changed the magnification factor of the unstable resonator to 10, 20, 40 and 60. The beam diameter was 20 mm and the discharge length was 80 cm.

The photograph of the fringes at the magnification factor of 60 is shown in Fig. 2. We read the inferference fringes by an image sensor and analysed them using a computer.

3.1. Data processing

The distribution of the intensity of the CVL beam is not uniform. To avoid the effect of nonuniformity, we employed the Fourier transform method of the fringe data processing by Takeda *et al.* [12].

The interference fringe $g(x)$ is

$$g(x) = a(x)[1 + |\gamma(x)| \cos \{2\pi f_0 x + \psi(x)\}], \tag{2}$$

where $a(x)$ is the light intensity distribution, $|\gamma(x)|$ is the modulation of the interference fringe modulation and f_0 is the spatial carrier frequency which is determined by the tilt angle between interfering two planes. The complex function, $\gamma(x) = |\gamma(x)| \exp(i\psi(x))$, is the complex degree of coherence.

We calculate the spatial spectrum of this fringe by Fourier transforms, given by

$$G(f) = A(f) + B(f - f_0) + B^*(f + f_0) \tag{3}$$

where

$$A(f) = F(a(x)),\ B(f) = F(a(x)\gamma(x))$$

and F stands for Fourier transform.

We set the spatial carrier frequency f_0 twice higher than the spectral width of $A(f)$ and $B(f - f_0)$, so that $A(f)$ and $B(f - f_0)$ do not overlap on the spectrum $G(f)$. Therefore we can get $a(x)$ by calculating the inverse Fourier transform of $A(f)$, and we can get $a(x)\gamma(x)$ by shifting the spectrum $B(f - f_0)$ by the carrier frequency f_0 and calculating the inverse Fourier transform of $B(f)$. The distribution of the fringe modulation $|\gamma(x)|$ can be calculated by dividing $a(x)\gamma(x)$ by $a(x)$ and taking the absolute value.

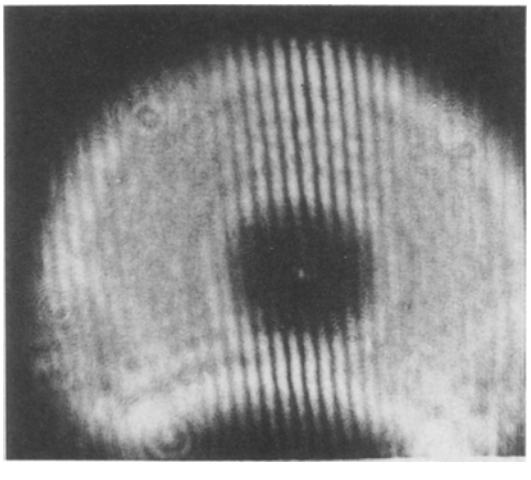

Figure 2 The photograph of the interference fringes of the CVL beam by the reversal shear interferometer. The beam pattern of the CVL beam is annular because the output coupler has a central hole.

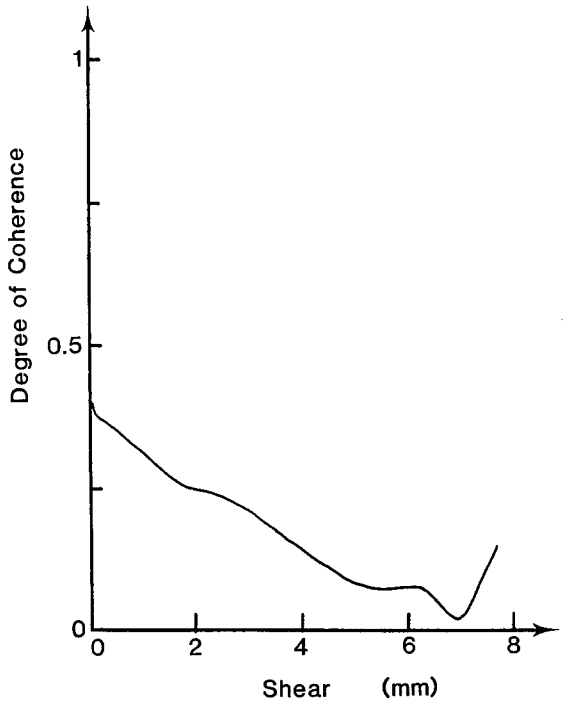

Figure 3 The coherence function of the CVL beam measured by the reversal shear interferometer. The magnification factor of the unstable resonator is 60.

3.2. Result

The result at the magnficiation factor of 60, of the unstable resonator is shown in Fig. 3. Because it was difficult to verify experimentally the shear at which the fringes vanish, we defined the coherence width as the shear, at which the visibility decreased down to 0.1 for the first time as increasing the shear. The quality of the spatial coherence function is evaluated by the coherence width. For the data in Fig. 3, the coherence width was about 5 mm. Similarly we measured the coherence width at the magnification factor of 10, 20 and 40. The result is listed in Table I. The maximum laser power was almost constant for different magnification factors. The higher the magnification factor, the larger the coherence width.

The spatial coherence was also measured by Young's interferometer for comparison at magnification of 60. The diameter of the pinholes were 50 μm. The result was shown in Fig. 4. The coherence width was about 5 mm.

TABLE I The measurement result of the coherence width of the CVL beam at various magnification factors of the unstable resonator.

Magnification factor of unstable resonator	Coherence width (mm)	Maximum laser power (W)
10	<2	1.8
20	2.8	1.8
40	4.2	1.8
60	5.0	1.9

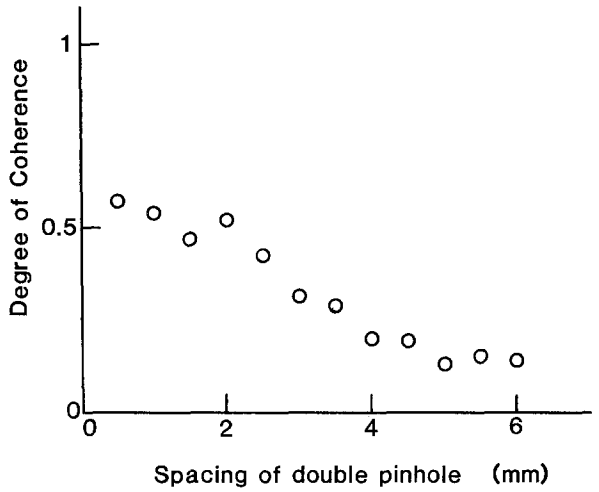

Figure 4 The coherence function of the CVL beam measured by the Young's interferometer. The magnification factor of the unstable resonator is 60.

The experimental result of the spatial coherence width obtained using our method agreed with that obtained by Young's interferometer.

4. Discussion

Since the CVL has a high gain coefficient, the spontaneous emission is amplified strongly during a round trip in the laser medium. The spontaneous emission, which propagates in the left direction in Fig. 5, is reflected at the output coupler and its outer part goes out of the resonator. It becomes the first part of the output pulse but the intensity is very low because the amplification is not enough. The emisison, which propagates in the right direction, is reflected at the concave mirror, goes back into the laser tube and is amplified again. Its outer part through the coupler goes out of the resonator and becomes the second

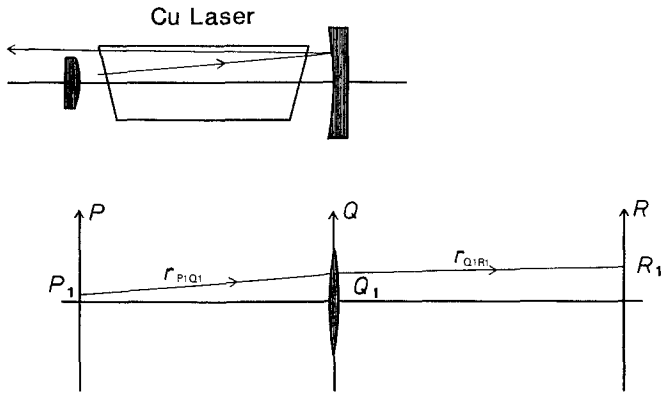

Figure 5 (a) The model for the calculation of the coherence function of the ASE. The propagation of the spontaneous emission in the lens system (b) is equivalent to the propagation of the spontaneous emission shown in (a). The point P_1 is on the left end of the laser tube. The point Q_1 is on a convex lens. The point R_1 is the observation plane.

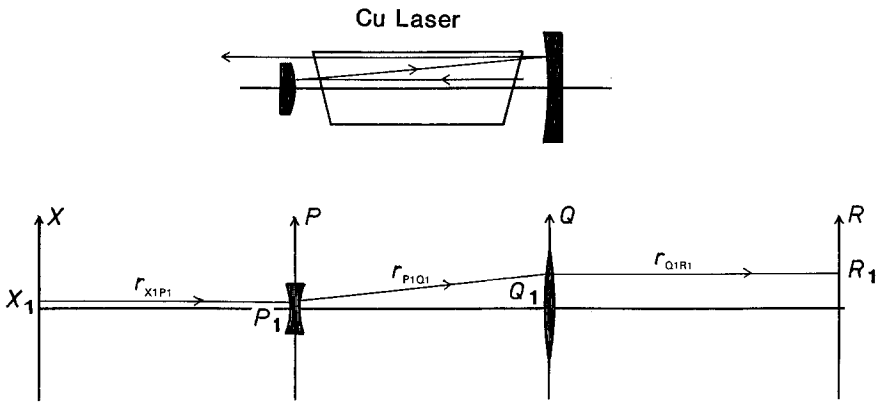

Figure 6 (a) The model for the calculation of the coherence function of the laser mode. The propagation of the spontaneous emission in the lens system (b) is equivalent to the propagation of the spontaneous emission shown in (a). The point X_1 is on the right end of the laser tube. The point P_1 is on the concave lens. The point Q_1 is on the concave lens. The point R_1 is the observation plane.

part of the output pulse. Since these parts of the output pulse do not propagate via the convex mirror, we call them the amplified spontaneous emission (ASE). The second part of the output pulse is a dominant of the ASE. This situation is shown in Fig. 5.

The inner part of the spontaneous emission, which propagates in the left direction, transmits the central hole of the output coupler, is reflected at the convex mirror and goes back to the laser tube. Then it is reflected at the concave mirror, returns to the laser tube again and its outer part finally goes out of the resonator. It becomes the third part of the output pulse power. Similarly the emission, which goes back and forth in the resonator, forms the fourth and later parts of the output pulse successively until the laser amplification terminates. We call them a laser mode. The third part of the output pulse is a dominant of the laser mode. This situation is shown in Fig. 6.

Since the spontaneous emission radiated from the active medium can be treated as the incoherent light, the mutual intensity of the ASE and the laser mode can be written using the von Cittert-Zernike theorem [8],

$$J_{12(\mathrm{ASE})}(R_1, R_2) = \langle u(R_1)u^*(R_2)\rangle$$
$$= B\int_P\int_Q\int_Q |u(P_1)|^2 \exp\{ik(r_{P1Q1} + r_{Q1R1})\}\exp\{-ik(r_{P1Q2} + r_{Q2R2})\}$$
$$\times K_2(Q_1)K_2^*(Q_2)\,\mathrm{d}P_1\,\mathrm{d}Q_1\,\mathrm{d}Q_2 \tag{4}$$

where we used the relation $\langle u(P_1)u^*(P_2)\rangle = \delta_{P1P2}$, $K_2(Q_1) = \exp(-ikQ_1^2/2f_2)$ is the phase shift at the concave mirror, k is wave number of the laser beam and $u(x)$ is the amplitude of the incoherent light source.

On the assumption that the intensity of the light source is uniform, we have

$$\int_P |u(P_1)|^2 \exp\{ik(r_{P1Q1} - r_{P1Q2})\}\,\mathrm{d}P_1 = C\,\mathrm{sinc}\{ka(Q_1 - Q_2)/Z_1\}\exp(i\phi) \tag{5}$$
$$\phi = k(Q_1^2 - Q_2^2)/2Z_1$$

where a is the diameter of the incoherent light source and Z_1 is the distance from the end of the active medium to the concave mirror.

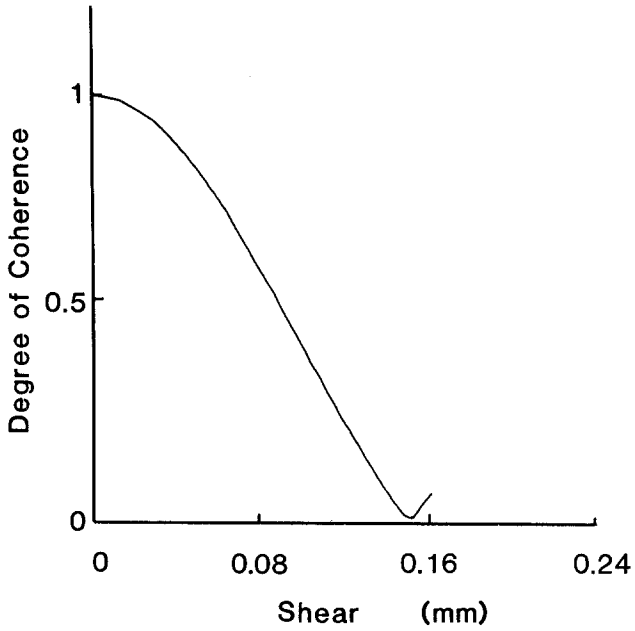

Figure 7 The coherence function of the ASE. The coherence width is 0.15 mm.

The degree of coherence $|\gamma_{12(\mathrm{ASE})}(R_1, R_2)|$ can be calculated by substituting Equation 5 into 4 and normalizing the Equation 4 with $J_{11(\mathrm{ASE})} = \langle u(R_1)u^*(R_1)\rangle$ and $J_{22(\mathrm{ASE})} = \langle u(R_2)u^*(R_2)\rangle$.

$$|\gamma_{12(\mathrm{ASE})}(R_1, R_2)| = |J_{12(\mathrm{ASE})}(R_1, R_2)/(J_{11(\mathrm{ASE})}J_{22(\mathrm{ASE})})^{1/2}| \tag{6}$$

The result of the calculation is shown in Fig. 7.

Similarly,

$$J_{12(\mathrm{laser})}(R_1, R_2) = \langle u(R_1)u^*(R_2)\rangle$$

$$= B' \int_X \int_P \int_P \int_Q \int_Q |u(X_1)|^2 \exp\left[ik\{(r_{X1P1} + r_{P1Q1} + r_{Q1R1}) - (r_{X1P2} + r_{P1Q2} + r_{Q2R2})\}\right]$$

$$\times K_1(P_1)K_1^*(P_2)K_2(Q_1)K_2^*(Q_2)\,\mathrm{d}X_1\,\mathrm{d}P_1\,\mathrm{d}P_2\,\mathrm{d}Q_1\,\mathrm{d}Q_2 \tag{7}$$

where $K_1(P_1)$ $(=\exp(ikP_1^2/2f_1))$ is the phase shift at the convex mirror.

We calculated Equation 7 similarly.

The result of $|\gamma_{12(\mathrm{laser})}(R_1, R_2)|$ is shown in Fig. 8. We defined the coherence width as the shear at which the visibility becomes zero. The coherence width of ASE (0.15 mm) was much smaller than that of the laser mode (4.5 mm). The coherence width of the laser mode agreed with the results of our experiments.

In any light source, the visibility should be unity at the shear zero. But the observed visibility was about 0.5.

The spatial resolution limit of our method is determined by the carrier frequency of the fringes. In our experiment, the carrier frequency was 2 lines mm^{-1} and the spatial resolution limit was about 0.5 mm. Because the coherence width of the ASE is smaller than the spatial resolution limit, the ASE becomes an incoherent uniform background light of the laser mode. Therefore we could not observe unit visibility at zero shear.

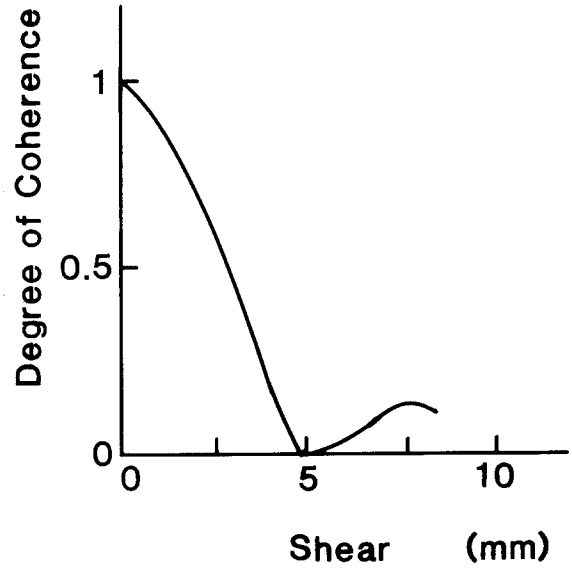

Figure 8 The coherence function of the laser mode. The coherence width is 5 mm.

5. Conclusion

We measured the spatial coherence of the CVL with the unstable resonator using the reversal shear interferometer. We could evaluate the spatial coherence function by a single-shot measurement.

The spatial coherence width of the CVL was 5.0 mm when the magnification factor 60 of the unstable resonator was used.

We verified the results of our experiment by the theoretical calculation on the basis of the passive resonator model.

References

1. W. T. WALTER, N. SOLIMENE, M. PILTCH and G. GOULD, *IEEE J. Quantum. Electron.* **QE-2** (1966) 474.
2. A. A. ISAEV, G. YU. LEMMERMAN and G. L. MALAFEEVA, *Sov. J. Quantum. Electron.* **10** (1980) 983.
3. K. KURODA, T. OMATSU, T. SHIMURA, M. CHIHARA and I. OGURA, *Proc. SPIE* **1041** (1989) 60.
4. D. W. COUTTS, M. D. AINSWORTH and J. PIPER, *IEEE J. Quantum. Electron.* **QE-25** (1989) 1985.
5. R. S. HARGROVE, R. GROVE and T. KAN, *IEEE J. Quantum. Electron.* **QE-15** (1979) 1228.
6. N. A. LYABIN, *Sov. J. Quantum. Electron.* **19** (1989) 426.
7. M. AMIT, S LAVI, G. EREZ and E. MIRON, *Opt. Commun.* **62** (1987) 110.
8. M. BORN and E. WOLF, Principles of Optics (MacMillan, New York, 1964) p. 260.
9. M. V. R. K. MURTY, *J. Opt. Soc. Am.* **50** (1960) 83.
10. A. R. GANESAN, D. K. SHARMA and M. P. KOTHIYAL, *Appl. Opt.* **27** (1988) 4731.
11. A. E. SIEGMAN, *Proc. IEEE* **53** (1965) 277.
12. M. TAKEDA, H. INA and S. KOBAYASHI, *J. Opt. Soc. Am.* **72** (1982) 156.